

Available online at www.sciencedirect.com**ScienceDirect**

Energy Procedia 91 (2016) 128 – 137

Energy

Procedia

SHC 2015, International Conference on Solar Heating and Cooling for Buildings and Industry

Thermochemical heat storage – from reaction storage density to system storage density

Ard-Jan de Jong^{a*}, Laurens van Vliet^a, Christophe Hoegaerts^a, Mark Roelands^a, Ruud Cuypers^a^aTNO, Leeghwaterstraat 44, 2628 CA Delft, The Netherlands

Abstract

Long-term and compact storage of solar energy is crucial for the eventual transition to a 100% renewable energy economy. For this, thermochemical materials provide a promising solution. The compactness of a long-term storage system is determined by the thermochemical reaction, operating conditions, and system implementation with the necessary additional system components. Within the MERITS project a thermochemical storage (TCS) system is being demonstrated using evacuated, closed TCS modules containing Na₂S as active material. The present modules are expected to reach a heat storage density of 0.18GJ/m³. In this paper, we discuss the different factors leading to this storage density, and argue that by further optimization of the selected reaction and architecture, the result may be improved to approximately 1GJ/m³, which would be a practical value for seasonal heat storage in buildings.

© 2016 The Authors. Published by Elsevier Ltd. This is an open access article under the CC BY-NC-ND license (<http://creativecommons.org/licenses/by-nc-nd/4.0/>).

Peer-review by the scientific conference committee of SHC 2015 under responsibility of PSE AG

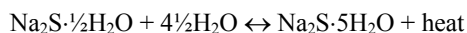
Keywords: thermochemical heat storage; energy storage; thermochemical materials; hygroscopic salts; heat storage density

1. Introduction

The eventual transition to a 100% renewable energy economy will largely rely on instantaneously captured solar energy, as other resources of renewable energy require unrealistic land use (cf. [1]), except for a few locations such as Iceland and Aruba. But as solar energy strongly fluctuates during the day and during a year, it will be necessary

* Corresponding author. Tel.: +31-(0)8886-64085; fax: +31-(0)8886-63023.
E-mail address: ardjan.dejong@tno.nl

to store large amounts of it during periods of up to at least half a year. A significant part of energy to be stored is for space heating and domestic hot water for buildings. Daily storage can be arranged by mature boiler technology, but seasonal storage for at least half a year will require considerably lower heat losses. Besides, seasonal heat storage will usually imply storing very large amounts of heat, so that heat storage should be compact, with high storage density. Energy storage by using solar heat (e.g. at 60–140°C) to reverse chemical reactions is an attractive solution, as the reaction products can be stored virtually loss-free. One example of a reaction suited to the given range of operating temperatures is:



The reaction heat storage density is about 2.9GJ per m³ of the hydrated salt Na₂S·5H₂O [2]. This is considerably lower than typical values of fossil fuels, which is inherent to the fact that the reaction runs at much lower temperatures, according to Trouton's rule [3]. The reaction storage density sets an upper limit to the storage density of any thermochemical storage (TCS) system, which will besides the thermochemical material (TCM) also need additional components, such as tubing, vessel, heat exchangers (HXs), and so on.

As a guideline for application in buildings, we aim for a system heat storage density of 1GJ/m³, so that a typical amount of 10GJ needed for heating a well-insulated dwelling in winter would fit in about 10m³. This implies that about 1/3 of the system volume should be TCM only, in case of the above Na₂S reaction. For the MERITS project, which will be discussed in Section 2, we implemented a modular TCS system for which the modules will reach a heat storage density of about 0.18GJ/m³. In Section 3, we discuss the different contributions leading to this number and argue that by further engineering, this number could be increased towards the objective 1GJ/m³.



Fig. 1. MERITS system at Universitat de Lleida (UDL).

2. MERITS

2.1. System and components

One of the main objectives of the FP7 project MERITS is to demonstrate a TCS system based on hydration and dehydration of a hygroscopic salt. Earlier, e.g. for the FP7 project E-hub (cf. [4]), reversible heat storage and delivery had been demonstrated using hydration and dehydration reactions of porous materials such as silica gel and zeolite. These materials are very stable and suited for lab experiments with cycles of actual heat delivery and storage, but show no perspective for application in buildings due to the low reaction heat storage density of around 0.1GJ/m³, which is already 10 times lower than the objective 1GJ/m³ on system level. For MERITS, we selected Na₂S due to its favorable operating temperatures, absence of deliquescence below 83°C (cf. [2]), promising behavior during cycles of hydration and dehydration, and because a lot is already known about it. This includes the drawback of possible H₂S formation by side reaction with H₂O (cf. [5]), and one of our targets was to prevent this by controlling operating conditions including corrosion control [6]. After the first lab tests, a first TCS module based on Na₂S was realized and demonstrated for several cycles of hydration and dehydration. During these initial tests, a

system heat storage density of 0.14GJ/m^3 was demonstrated. During coming demonstration tests the modules are estimated to reach 0.18GJ/m^3 . Fig. 1 shows the MERITS system. This is a complete storage system and building simulation compartment in a 45ft container. Field test demonstrations were already carried out in Lleida during the past summer without TCM storage, and are planned in Warsaw in the beginning of 2016 with TCM storage.

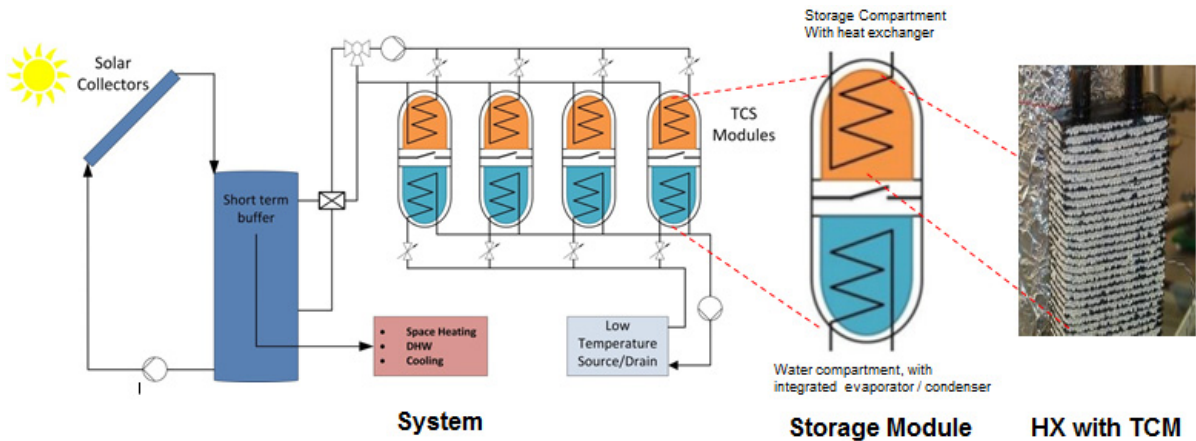


Fig. 2. MERITS system architecture and components.

We will now sketch components and operation based on Fig. 2. During the warm season, excess heat from the solar collectors of about 80°C is transferred via a short term buffer vessel to a heat storage module. This module contains the TCM in the hydrated state $\text{Na}_2\text{S}\cdot 5\text{H}_2\text{O}$ (orange) which is dried to $\text{Na}_2\text{S}\cdot \frac{1}{2}\text{H}_2\text{O}$, while the removed process water (blue) is captured in the condenser. Prior to operation, the module is evacuated, so that water vapor should be the only present gas. The dry salt is stored for later use during the cold season. Then, $\text{Na}_2\text{S}\cdot \frac{1}{2}\text{H}_2\text{O}$ is hydrated with the process water and the stored heat is recovered. The evaporator/condenser of a module is connected to a low temperature source/drain. In reality, this could be a borehole thermal energy storage. For the MERITS demonstrator, this part is replaced by a laboratory water bath.

Thus, the MERITS architecture implements a closed, vacuum system, composed of a number of identical modules, each containing a fixed TCM bed in a HX and the required amount of process water with a second HX. This concept has many advantages. For instance, vacuum ensures rapid evaporation, condensation and vapor transport (at the speed of sound, since vapor concentration gradients are then pressure gradients). Besides, a modular setup is favorable for scalability. However, a fixed bed architecture is not optimal regarding heat storage density, because each module requires a separate vessel, and HXs for TCM and process water. Instead, one might consider adopting a moving bed architecture with a single central HX, which is periodically filled with TCM from a single, large storage tank containing only TCM (cf. [7]). This would increase system heat storage density close to the value of the TCM storage tank, particularly for larger amounts of stored heat. However, this architecture introduces the challenge of reliable, repeated TCM transport between a central HX and a TCM storage tank. For MERITS, we have therefore chosen not to further pursue this concept in favor of a fixed bed concept.

2.2. Storage density compared to other systems

Table 1 compares the heat storage density of 0.18GJ/m^3 for the MERITS system to alternative energy storage systems. We see that the MERITS result is already an improvement with respect to the heat storage density of hot water tanks storing at 90°C and delivering at 50°C . However, a hot water tank is not well-suited for seasonal storage, as illustrated by Fig. 3, which is evaluated for a tank with 6cm insulation with a thermal conductivity of $\lambda = 0.04\text{W/mK}$. We note that heat storage in phase change materials would be somewhat more compact than hot water (cf. [8]), but deals with similar thermal heat losses.

Table 1. Storage densities, losses and costs of several heat storage systems.

Storage type	Volume [m ³]	Q/V [GJ/m ³]	Q ($t=0$) [MJ]	Q ($t=6m$) [MJ]	Costs [€/MJ]
Hot water tank	2.7	0.13	344	~0	~0.4
MERITS TCS	2.7	0.18	480	480	~5
Li-ion battery	2.7	1.6	~4400	~2300	~111

Li-ion batteries (cf. [9]) have higher energy storage density and perhaps acceptable losses in 6 months, but are inherently much more expensive than TCS systems, because Lithium is much more expensive than hygroscopic salts such as Na₂S. For better comparison, we add that stored electric energy may be converted to heat of 60°C by an electric heat pump with a coefficient of performance of COP = 2-3, improving storage density and costs by the same factor. From Table 1 we conclude that the MERITS system already has a significant performance improvement over hot water storage and has much better cost perspectives than rechargeable batteries. And as we will discuss below, there are good perspectives to further improve on the present result.

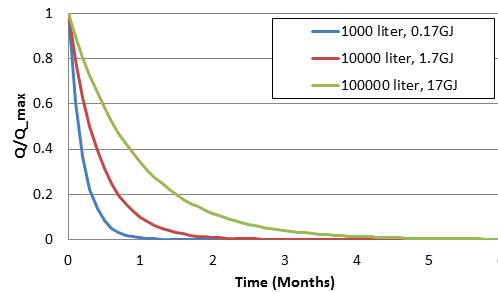


Fig. 3. Heat losses of a hot water storage tank.

3. From reaction to system heat storage density

3.1. Reaction heat storage density

The heat storage density of a given hydration reaction $H \rightarrow D + nH_2O$ is given by:

$$\frac{Q}{V} = \rho_H \frac{Q}{m} = \frac{\rho_H}{M_H} \Delta h_r = \frac{\rho_H}{M_H} n \Delta h_w \quad (1)$$

Here, the subscripts H and D refer to hydrated and dehydrated states, Q/V [J/m³], Q/m [J/kg], Δh_r [J/mol] are the reaction heat storage densities per volume, mass and mole, ρ_H [kg/m³] and M_H [kg/mol] are density and molar mass of the hydrated state, which will have highest volume, and Δh_w [J/mol] is the reaction enthalpy per mole water. For application to a TCS system, we also need the temperatures at which hydration and dehydration occurs. These follow from the Van 't Hoff's equation for a vapor pressure line (or pT-line):

$$\ln \frac{p}{p_0} = \frac{\Delta h_w}{R} \left[\frac{1}{T_0} - \frac{1}{T} \right] \quad (2)$$

This holds around a reference point (T_0, p_0) on the pT-line. As an example, Fig. 4 shows the pT-lines of Na₂S hydration reactions, where the numbers 1/2, 2, 5, 9 refer to the number of water molecules per Na₂S molecule. Now suppose that Na₂S·5H₂O is dried with the condenser at $T_C = 20^\circ\text{C}$, giving a vapor pressure of $p_C = 23\text{mbar}$. At this vapor pressure, drying to Na₂S·1/2H₂O is possible at about $T_D = 80^\circ\text{C}$, according to the pT-line of the 2-1/2 transition. Conversely, when heat is released by hydration with water from an evaporator at $T_E = 10^\circ\text{C}$, sorption heat by the formation of Na₂S·5H₂O can be delivered up to about $T_S = 65^\circ\text{C}$, according to the pT-line of the 5-2 transition. Note that these are limiting cases at low, quasi-stationary power delivery. For the given reaction, we have $h_r = 308\text{kJ/mol}$

[2], $\rho_H = 1580 \text{ kg/m}^3$ and $M_H = 0.168 \text{ kg/mol}$, so that (1) yields a reaction heat storage density of $Q/V = 2.9 \text{ GJ/m}^3$. This, then, is the upper limit for system heat storage density for the given reaction.

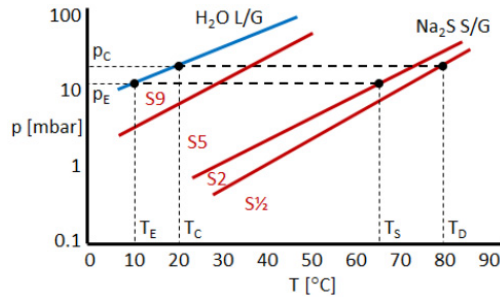


Fig. 4. Linearized pT-diagram of Na_2S hydration reactions (after [2]).

3.2. Process water

For a closed system such as the MERITS system of Fig. 2, all process water needs to be included. This process water already enlarges the system and thus reduces the maximally achievable system storage density. Table 2 gives the heat storage densities of several reactions with and without process water.

Table 2. Heat storage densities and operating conditions for several reactions for $T_E = 10^\circ\text{C}$, $T_C = 20^\circ\text{C}$.

Reaction	T_S [$^\circ\text{C}$]	T_D [$^\circ\text{C}$]	Q/V [GJ/m^3]	$Q/(V_H+V_W)$ [GJ/m^3]
$\text{Na}_2\text{S} \cdot \frac{1}{2}\text{H}_2\text{O} + 4\frac{1}{2}\text{H}_2\text{O} \leftrightarrow \text{Na}_2\text{S} \cdot 5\text{H}_2\text{O}$	65	80	2.9	1.6
$\text{SrBr}_2 \cdot \text{H}_2\text{O} + 5\text{H}_2\text{O} \leftrightarrow \text{SrBr}_2 \cdot 6\text{H}_2\text{O}$	45	52	1.9	1.2
$\text{CaCl}_2 \cdot 2\text{H}_2\text{O} + 4\text{H}_2\text{O} \leftrightarrow \text{CaCl}_2 \cdot 6\text{H}_2\text{O}$	35	52	1.8	1.2
$\text{MgCl}_2 \cdot 2\text{H}_2\text{O} + 4\text{H}_2\text{O} \leftrightarrow \text{MgCl}_2 \cdot 6\text{H}_2\text{O}$	60	110	1.9	1.2

Storing process water might be avoided by an open system, where process water is supplied externally, e.g. from deaerated and purified tap water or from ambient air (cf. [10]). In the latter case, one may also try to extract evaporation heat from ambient air. This, however, is particularly unfavorable during winter when air is cold and dry.

3.3. Insulation

For heat storage, TCM modules just need to be kept dry at ambient temperature, but we still deal with thermal insulation of the TCM module that is being used for sorption heat production (e.g. at 60°C) or for desorption heat storage (e.g. at 80°C). This insulating material adds to system volume and contributes to system heat storage density. We will show here that this insulation issue can be effectively handled by constraint optimization of the system heat storage density q_{sys} [J/m^3], which we define as:

$$q_{\text{sys}} \equiv \frac{Q_0}{V_{\text{sys}}} = \frac{Q_s - Q_l}{V_{\text{sys}}} \quad (3)$$

Here, Q_0 [J] is the heat released to the output HX, Q_s the produced sorption heat, Q_l the heat loss and V_{sys} the system volume including insulation. Another performance indicator is the heat loss fraction η :

$$\eta \equiv \frac{Q_l}{Q_0} \quad (4)$$

This η is determined by the thickness b and the thermal conductivity λ of the insulation. Now by assuming a certain packing geometry of modules with a certain internal heat storage density q , one can compute the necessary

number of modules N as well as the system heat storage density q_{sys} as a function of module dimension L and heat loss fraction η . This procedure is a bit lengthy but straightforward and worked out in Appendix A for the cubic module and system geometry of Fig. 5a. The resulting heat storage density for $Q_0 = 10\text{GJ}$, $q = 1.5\text{GJ/m}^3$ and $\lambda = 0.04\text{W/mK}$ is shown in Fig. 5b, and the required number of modules is given in Fig. 5c. For instance, for $\eta = 0.2$, $N = 64$ modules of $L = 50\text{cm}$ will do, giving an operating time of about 2 days per module (see Appendix A). Note that according to Fig. 5b, smaller modules lead to higher q_{sys} . This may seem contra-intuitive, as heat losses as usually reduced by decreasing the surface to volume ratio (which goes with $1/L$) i.e. by increasing module size. However, in our case only one of the operating modules is at operating temperature and needs to be insulated. So the surface to be insulated is $6L^2$ (for cubic modules), and this is minimized by reducing L . On the other hand, reducing L means increasing power density, and this can only be done until a certain power peaking limit, regarding material degradation. This is illustrated by Fig. 5d, where a fictive black line indicates maximum power density.

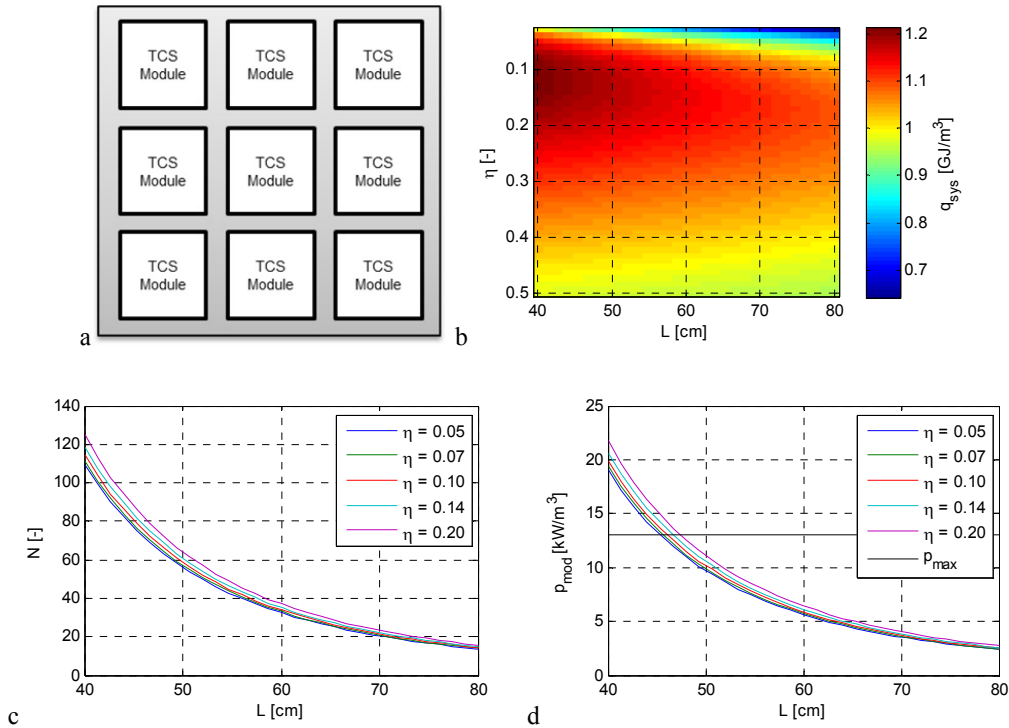


Fig. 5. (a) elementary system geometry (b) heat storage density (c) number of modules (d) power density.

Note that in this case, decreasing η only helps increasing q_{sys} until about $\eta = 0.12$, which may be explained by the fact that very small η requires very thick insulation, increasing the amount of inert material in the system. Fig. 5b indicates that for optimal packing, q_{sys} can be as high as about 80% of q with optimal insulation. For the current modules, about 25% of the module volume is insulation. We add that the inert volume fraction due to insulation could be further reduced by reducing λ , e.g. by vacuum insulation, which has a typical λ of 0.007W/mK .

3.4. Physical and chemical stabilization

An ideal TCM would not deteriorate during cycling at operation temperatures, i.e. would not have any chemical side reactions, possibly enabling corrosion, would not pulverize, would not have deliquescence issues and so on. However, as far as we know, all hygroscopic salts that have been dealt with so far are sensitive to some cycling instability issues, and therefore several ways of TCM stabilization have already been considered. Matrix encapsulation, i.e. including the TCM inside a stable porous matrix, seems to be the most commonly considered

solution. Several matrix materials have been considered, some with interesting side benefits. Naturally expanded graphite (NEG) has the perspective of additionally increasing thermal conductivity (cf. [5]). Zeolite and silica gel have the advantage that they also store some heat (cf. [11, 12]). The porous structure may have some influence on TCM thermodynamics (cf. [13]).

For MERITS, we studied stabilization with polymers [14], with the main purpose to have a flexible additive dealing with the considerable volume changes of about a factor 2.5 for the Na_2S transitions between $\frac{1}{2}$ and 5 hydrates. It is difficult to predict the minimum amount of stabilizing additive. Ideally, pure TCM crystals reach a stable state automatically after several successive cycles of hydration and dehydration, as for instance observed for BaCl_2 [15]. What may have happened in this case is illustrated by Fig. 6, showing an example of a macro-crystal, which is cracked during one of our cycling experiments. If such a cracked structure would be found to hold stable for a promising TCM, with sufficient vapor and heat transport, no additional stabilizing material would be needed, and we just deal with the packing density of e.g. $\pi/3\sqrt{2} \cong 0.74$ for spherical grains.

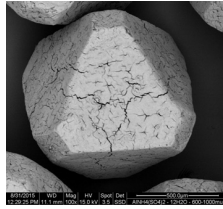


Fig. 6. Macro-crystal with cracks due to cycles of hydration and dehydration.

3.5. Enhancement of vapor and heat transport

Output power, which is an additional performance indicator besides heat loss and heat storage density, may also demand for TCM additives. Output power is limited by vapor and heat transport at crystallite, grain and bed levels, with corresponding dimensions L_C , L_G and L_B , as illustrated by Fig. 7, where a is crystal lattice spacing. One may include reactor level, in case the reactor is build up from units of TCM beds.

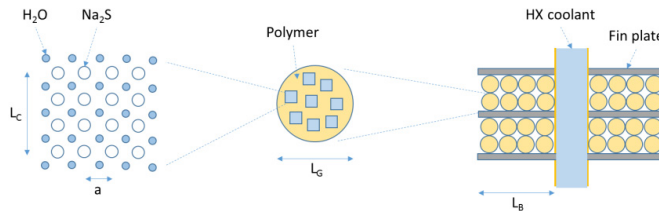


Fig. 7. Composite TCM – Crystallite (C), Grain (G) and Bed (B) levels.

With quantified models of vapor and heat transport at different levels, TCM dimensions of different levels can be optimized. For instance, if vapor and heat transport can be characterized by diffusion constants D_j [m^2/s] and α_j [m^2/s] respectively, then a stationary output power P is produced at all TCM levels in the reactor:

$$P = \frac{\Delta h}{M} A_j J_j \cong \frac{\Delta h}{M} A_j D_j \gamma_j \frac{\Delta n_j}{L_j} \equiv \frac{\Delta n_j}{R_j} \quad (5)$$

Here, A_j [m^2] and J_j [$\text{m}^{-2}\text{s}^{-1}$] are interface area and vapor flow density, and Δn_j is the concentration difference over the effective transport distance L_j/γ_j , where γ_j is a geometrical factor. For convenience, we defined a transport resistance R_j , similar to Ohm's law. With that, the stationary output power P flowing through all levels reads:

$$P = \frac{\sum_j \Delta n_j}{\sum_j R_j} \quad (6)$$

It follows that stationary power for a given total concentration difference is maximized by minimizing the sum of the resistances as a function of the geometric parameters L_j , A_j , γ_j for given D_j and TCM geometry. In practice, optimization may come down to estimating Δn_j for all levels, allowing to identify bottlenecks with large Δn_j , and modify TCM geometry to reduce these particular Δn_j . Besides, heat transport must keep pace with vapor transport, so that similar considerations must be followed with α_j and temperature differences ΔT_j instead of D_j and Δn_j .

If no satisfactory TCM dimensions are obtained, a different type of TCM has to be considered, or the selected TCM has to be enhanced. This could be done on micro or nanoscale, but for MERITS, vapor and heat transport were enhanced on mm-scale using a HX similar to the picture on the right of Fig. 2. This HX has an inert volume fraction of about 20%. In principle, this volume fraction could be avoided by TCM with already satisfactory transport properties. Moreover, the current $\text{Na}_2\text{S} \cdot 5\text{H}_2\text{O}$ bulk density in MERITS modules is about 0.6kg/m^3 , which is only about 37% of value of 1.58kg/m^3 for crystallites. How much porosity is needed for vapor transport depends on transport parameters. Reserving 25% of bulk porosity for vapor transport would allow increasing Na_2S bulk density in MERITS modules by a factor 2.

3.6. Internal components influencing the storage density

As shown in Fig. 2, the Merits TCS modules exist of a low pressure vessel containing as main components the heat exchanger with the TCS material, the internal valve and the condenser/evaporator combined with the process water and tubing. All internal components have to be fitted within the shape of the vessel, which will give losses due to non-ideal fit factors. For the MERITS project a trade-off had to be made between development time, costs and performance. This process led to the selection of commercial available heat exchangers that were coated against corrosion [6]. Currently rectangular shaped heat exchangers are used, while the vessels have a circular cross-section. This combination resulted in the fact that only a relative small fraction (~50%) of the cross sectional area of the vessel is filled with heat exchangers and so with TCS material. So a significant increase in performance can be expected in the future when better fit factors will become available. Another point of loss is space required to lead the internal tubing towards a single input and output connection. Optimization of the design and size of the internal valve, required to enable the seasonal storage, also will influence the storage capacity of the modules. When modules in the future will be scaled to larger storage capacity the scaling in itself will have positive effect on all the loss factors mentioned above.

3.7. Recapitulation

The above considerations may be wrapped up by the following formula for system heat storage density:

$$\frac{Q}{V} = \frac{Q_0 \beta_0}{V_1 \beta_1 + V_2 \beta_2 + V_3 \beta_3} \quad (7)$$

Here, Q_0 is the amount of stored heat, V_1 , V_2 , V_3 are reactor, evaporator and insulation volumes per module (See Fig. 2, V_1 orange, V_2 blue and V_3 is a layer of insulation around the module) and β_0 , ..., β_3 are improvement factors with respect to the MERITS result with $\beta_0 = \dots = \beta_3 = 1$. As shown in Table 3, we expect largest gain in β_0 , containing enlarged Na_2S bulk density and optimized packing of HXs in the module. We assume that the reactor volume remains the same, i.e. $\beta_1 = 1$. With more Na_2S , the process water and HX volumes increase proportionally, resulting in a factor $\beta_2 = 2.9$ for the evaporator. Finally we estimate a factor $\beta_3 = 1/5$ by optimizing insulation, leading to $Q/V = 0.81\text{GJ/m}^3$ for Na_2S for the given operating conditions and design consideration. This already closely approaches the objective value of 1GJ/m^3 .

Table 3. Estimated achievable system heat storage density improvement with respect to current MERITS module.

Reaction	$Q\beta_0$ [MJ]	$V_1\beta_1$ [l]	$V_2\beta_2$ [l]	$V_3\beta_3$ [l]	Q/V [GJ/m^3]
MERITS module	60	215	31	80	0.18
Estimated achievable improvement	261	215	90	16	0.81

4. Conclusions

TCS offers the potential of loss-free storage with a heat storage density higher than water. The first lab results of the MERITS project show that a storage density of 0.14 GJ/m^3 was achieved and we expect to reach 0.18 GJ/m^3 for coming field tests in the beginning of next year. Based on the experience obtained in MERITS, we identified a number of possible improvements of the storage density on the system level. In this paper we identified and analyzed a number of possible improvements, and show that by mere optimization of the MERITS fixed-bed reactor concept using Na_2S , a heat storage density of approximately 1 GJ/m^3 can already be achieved.

Acknowledgements

The research leading to these results has received funding from the European Commission Seventh Framework Programme (FP/2007-2013) under grant agreement No ENER/FP7/295983 (MERITS). MERITS is a R&D project supported by the European FP7 program with the aim to build a prototype of a compact rechargeable thermal battery. Such a product would offer a new solution for improved use of renewable sources for domestic heating, cooling and hot water appliances and thus greatly contribute to the European ambition of an energy-neutral built environment by 2050.

The project is carried out by four research institutes (TNO, VITO, Tecnalia, Fraunhofer ISE), two universities (Ulster University, University of Lleida), two SME's (De Beijer RTB, Zonne-Energie Nederland BV), and two industries (Mostostal, Glen Dimplex). The team will work with novel high energy density thermochemical materials that can supply required heating, cooling and domestic hot water for a dwelling with up to 100% renewable energy sources (e.g. the sun) throughout the year. The key development issues are:

- The delivery of heat on different dedicated temperature levels for heating, cooling and domestic hot water
- The tailoring to the requirements of individual dwellings
- The design and development of a dedicated solar collector
- The integrated design for the components and enhanced thermo-chemical materials, including the control system

Furthermore the project includes the development of business models and market strategies to foster market take-up before 2020. More information on MERITS is available on our public website “www.MERITS.eu”.

In addition, we wish to thank our colleagues Joris Salari and Hartmut Fischer for providing the picture of Fig. 6, used to illustrate our ideas about the influence of cycling on crystal structure, vapor and heat transport.

Appendix A. Insulation modeling

The needed amount of stored heat Q_0 can be written as the difference between sorption heat Q_s and heat loss Q_l :

$$Q_s - Q_l = Q_0 = P_0 t_0 \quad (\text{A1})$$

Here, P_0 is the average output power and t_0 is the time of heat delivery. For instance, with $Q_0 = 10 \text{ GJ}$, $t_0 = 100$ days, we have $P_0 = 1.2 \text{ kW}$. In order to estimate heat loss, some geometry of composite TCM and insulation must be chosen. We will assume the geometry of Fig. 5a with cubic modules of width L . The loss power reads:

$$P_l = hA(T_s - T_a) \quad (\text{A2})$$

Here, h [$\text{W/m}^2\text{K}$] is the heat transfer coefficient of the insulation, $A = 6L^2$ is the loss area, and T_s and T_a are sorption and ambient temperatures. The heat loss fraction can be defined as:

$$\eta \equiv \frac{Q_l}{Q_0} = \frac{P_l}{P_0} = \frac{hA(T_s - T_a)}{P_0} = \frac{6\lambda L^2(T_s - T_a)}{bP_0} \quad (\text{A3})$$

Here, we substituted $h = \lambda/b$, where λ [W/mK] is the insulation thermal conductivity and b is the insulation thickness. This η is an important performance indicator. The amount of stored sorption heat can be written as:

$$Q_s = NqV = NqL^3 \quad (A4)$$

Here, N is the number of modules and q [J/m³] the heat storage density per module of volume $V = L^3$. The number of modules needed for delivering Q_0 can now be expressed by:

$$N = \frac{Q_0}{qL^3} (1 + \eta) \quad (A5)$$

A perfectly cubic system of N insulated cubes has $N^{1/3}$ on each side, giving the following system width:

$$L_{sys} = N^{1/3} (L + b) + b \quad (A6)$$

Thus we find the following for system heat storage density:

$$q_{sys} = \frac{Q_0}{V_{sys}} = \frac{Q_0}{L_{sys}^3} = \frac{Q_0}{[N^{1/3} (L + b) + b]^3} \quad (A7)$$

This q_{sys} [J/m³] is another performance indicator besides η . In the above, we already showed plots of N , q_{sys} and power density for the case $Q_0 = 10$ GJ, $q = 1.5$ GJ/m³, $\lambda = 0.04$ W/mK. Figs A1a and A1b show the corresponding operation time per module and the required insulation thickness.

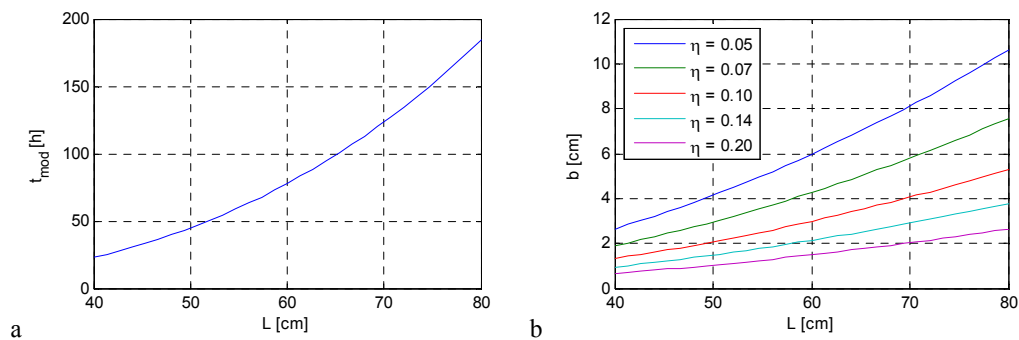


Fig. A1. (a) module operation time (b) insulation thickness.

References

- [1] Hermann, WA. Energy 2006;31:1685-1702.
- [2] De Boer, R, Haije, W, Veldhuis, JBJ. Thermochemica Acta 2003;395:3-19.
- [3] Trouton, F. Philosophical Magazine 1884;18:54-57.
- [4] Finck, C, Henquet, E, Van Soest, C, Oversloot, H, De Jong, AJ, Cuypers, R, Van't Spijker, H. Energy Procedia 2014;48:320-326.
- [5] Maura, S, Lahmidi, H, Goetz, V. Solar Energy 2008;82:623-636.
- [6] De Jong, AJ, Stevens, R, Rentrop, C, Hoegaerts, C. Energy Procedia 2015;70:182-192.
- [7] De Jong, AJ, Trausel, F, Finck, C, Van Vliet, L, Cuypers, R. Energy Procedia 2014;48:309-319.
- [8] Cot-Gores, J, Castell, A, Cabeza, LF. Renewable and Sustainable Energy Reviews 2012;16:5207-5224.
- [9] Panasonic. Datasheet NCR18650, Lithium ion, Version 13.11 R1 2012
- [10] Casey, SP, Elvins, J, Riffat, S, Robinson, A. Energy and Buildings 2014;84:412-425.
- [11] Simonova, IA, Aristov, YI. Russian Journal of Physical Chemical 2005;79:1307-1311.
- [12] Aristov, YI. Journal of Chemical Engineering of Japan 2007;40:1242-1251.
- [13] Steiger, M, Asmussen, S. Geochimica et Cosmochimica Acta 2008;72:4291-4306.
- [14] Roelands, M, Cuypers, R, Kruit, K, Oversloot, H, De Jong, AJ, Duvalois, W, Van Vliet, L, Hoegaerts, C. Energy Procedia 2015;70:257-266.
- [15] Andersson, J, Azoulay, M, De Pablo, J. Thermochemica Acta 1983;70:291-302.